On the phase speed and attenuation of an interface wave in an unconsolidated marine sediment

Michael J. Buckingham[a)]
Marine Physical Laboratory, Scripps Institution of Oceanography, University of California, San Diego, 9500 Gilman Drive, La Jolla, California 92093-0213

(Received 23 March 1998; accepted for publication 7 June 1999)

The phase speed and attenuation of the interface wave at the seawater–sediment boundary are obtained by solving the characteristic equation for one of its complex roots. The characteristic equation itself is derived on the basis of a recently developed theory of wave propagation in porous media. Central to the theory is the stress relaxation that occurs when mineral grains slide against one another during the passage of a seismic wave. This type of stress relaxation is characterized by material response functions for compressional and shear waves of the form $h(t) \propto t^{-n}$, where t is time since the sliding began and n is a small positive number. The phase speed of the interface wave relative to that of the shear wave depends weakly on the grain size, increasing from about 85% for fine-grained silts and clays to 90% for coarse sands. The loss tangent of the interface wave, β_i, is found to be independent of the mechanical properties (grain size, porosity, and density) of the sediment, and is the same as that for the shear wave: $\beta_i \approx 0.04$. Since the loss tangent and phase speed are, in effect, independent of frequency, the attenuation coefficient of the interface wave scales as the first power of frequency. It turns out that the characteristic equation for the interface wave, as derived from the intergranular stress-relaxation mechanism, is exactly the same as if the sediment had been treated as an elastic solid. However, the elastic description fails to account for the grain-size dependencies exhibited by the compressional and shear waves. These dependencies emerge naturally from the stress-relaxation model. [S0001-4966(99)00710-9]

PACS numbers: 43.20.Jr, 43.30.Ma, 43.30.Ky, 43.35.Mr. [DLB]

LIST OF SYMBOLS

j	$\sqrt{-1}$
c_p	compressional wave speed in sediment
c_s	shear wave speed in sediment
c_0	compressional wave speed in sediment in absence of intergranular stress relaxation
c_w	compressional wave speed in water column
c_i	interface wave speed
η_h	coefficient of shear stress relaxation
λ_h	coefficient of compressional stress relaxation
μ_c	compressional stress-relaxation rigidity modulus
μ_s	shear stress-relaxation rigidity modulus
ω	angular frequency
$k_0 = \omega/c_0$	compressional wave number in sediment in absence of intergranular stress relaxation
$k = \omega/c_p$	compressional wave number in sediment
$k_s = \omega/c_s$	shear wave number in sediment
$k_w = \omega/c_w$	compressional wave number in seawater
p	horizontal wave number
$s = k_s^2/p^2$	dimensionless variable in characteristic equation
$\eta = \sqrt{k^2 - p^2}$	vertical compressional wave number in sediment
$\eta_s = \sqrt{k_s^2 - p^2}$	vertical shear wave number in sediment
$\eta_w = \sqrt{k_w^2 - p^2}$	vertical compressional wave number in seawater
t	time
$h(t)$	compressional material response function
$h_s(t)$	shear material response function
$H(j\omega)$	Fourier transform of $h(t)$
$H_s(j\omega)$	Fourier transform of $h_s(t)$
ψ_w	velocity potential, compressional wave in water column
ψ	velocity potential, compressional wave in sediment
ψ_s	velocity potential, shear wave in sediment
n	exponent of compressional material response function ($0 < n < 1$)
m	exponent of shear material response function ($0 < m < 1$)
u_g	mean grain diameter, micrometers
ρ_0	density of sediment
$\rho_w = 1024\ \mathrm{kg/m^3}$	density of seawater
$\rho_g = 2700\ \mathrm{kg/m^3}$	density of mineral grains
$b = \rho_w/\rho_0$	density ratio
κ_0	bulk modulus of sediment

[a)]Also at: Institute of Sound and Vibration Research, The University, Southampton SO17 1BJ, England. Electronic mail: mjb@mpl.ucsd.ed

$\kappa_w = 2.25 \times 10^9$ Pa	bulk modulus of seawater
$\kappa_g = 1.47 \times 10^{10}$ Pa	bulk modulus of mineral grains
$\Delta = 3$ μm	rms grain roughness
$u_0 = 1000$ μm	reference grain diameter
$\mu_0 = 2 \times 10^9$ Pa	compressional stress-relaxation scaling modulus
$\mu_1 = 5.1 \times 10^7$ Pa	shear stress-relaxation scaling modulus
N	porosity of sediment
$P = 0.63$	packing factor of randomly packed, uniform spheres

INTRODUCTION

In a recent series of papers, Buckingham[1–4] has developed a theory of seismic wave propagation in unconsolidated and consolidated saturated granular media. Central to the theory are material response (or memory) functions of the form $h(t) \propto t^{-n}$, where the index n is positive and much less than unity. This type of material response function represents a particular form of stress relaxation, proposed as arising from the microscopic sliding that occurs at grain-to-grain contacts during the passage of a wave through the medium. According to the theory, the stress relaxation introduces rigidity into the medium,[2] which allows shear waves to propagate even though the elastic rigidity (or ''frame'') modulus of the material is taken to be identically zero. Moreover, the predicted seismic-wave attenuation is proportional to the first power of frequency, which is consistent with the measured attenuation of compressional and shear waves in both unconsolidated marine sediments[5–8] and consolidated, sedimentary rocks such as sandstone or limestone.[9]

A material that supports shear, whether associated with elasticity or stress relaxation, may also be expected to support an interface wave. The speed and attenuation of the interface wave will be governed by a characteristic equation that is determined from the boundary conditions. The purpose of this article is to derive the characteristic equation for an interface wave propagating along the boundary between an unconsolidated, porous sediment of the type discussed by Buckingham[1–4] and an overlying fluid (seawater). Complex solutions of this equation are developed which yield the interface wave speed and the attenuation coefficient.

Before proceeding with the discussion, it is appropriate to address a question of semantics. By the term ''interface wave,'' we mean the classical type of evanescent surface wave that propagates along the boundary between a homogeneous solid and: (1) a vacuum (Rayleigh wave); or (2) a fluid (Scholte wave); or (3) another solid (Stoneley wave). Such waves exist when the solid supports shear through elasticity. When the shear arises from stress relaxation rather than from elasticity, as is taken to be the case for the granular media considered below, the interface wave will be identified by the prefix ''pseudo.'' Thus, at the seawater–sediment boundary we shall refer to the ''pseudo-Scholte'' wave. This usage is not to be confused with terms such as ''pseudo-Rayleigh'' wave used by some authors[10] in connection with an interface wave seen at the boundary between an elastic solid and a thin layer of fluid.

Following Buckingham,[1–4] it is assumed in deriving the characteristic equation that the unconsolidated sediment possesses no elastic frame; that is to say, the elastic modulus of the material is taken to be zero. Stress relaxation, arising from grain-to-grain sliding, as discussed by Buckingham,[4] is considered to be the mechanism that gives rise to shear, dissipation, and the existence of the interface wave. The characteristic equation itself is a function of the variable s, which is defined as the ratio of the complex wave number of the shear wave to the complex wave number of the interface wave. Underpinning the analysis are the usual boundary conditions; that is, continuity of total stress and of normal component of particle velocity across the seawater–sediment interface. In the absence of attenuation in the granular medium, one root of the characteristic equation would be real. This root becomes complex when attenuation is included in the analysis. The attenuation coefficient and the phase speed of the pseudo-Scholte wave are derived by solving the characteristic equation for this complex root. As with the attenuation of the compressional and shear waves, the attenuation coefficient of the interface wave is found to scale linearly with frequency. Although experimental data on the attenuation of interface waves in marine sediments are scarce, a comparison is made with the few data sets that are available, from which it is evident that the theoretically predicted attenuation is consistent with the observations.

I. WAVE EQUATIONS AND MATERIAL RESPONSE FUNCTIONS

Figure 1 illustrates the geometry of the problem. A horizontal boundary representing the seafloor separates two infinite, homogeneous, isotropic half spaces, the lower being the unconsolidated sediment consisting of mineral grains and interstitial seawater and the upper a conventional fluid, in this case seawater. An impulse of momentum (e.g., a hammer blow) is applied at a point on the seabed. The resultant wave

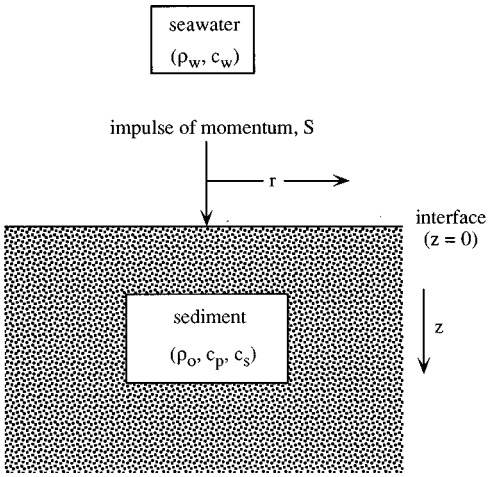

FIG. 1. Schematic showing the geometry of the fluid–sediment interface problem.

fields in both media are to be determined subject to the requirements that the stress and the normal component of particle velocity should be continuous across the interface.

The equation to be solved for the compressional wave field in the (assumed lossless) fluid above the boundary is

$$\nabla^2\Psi_w - \frac{1}{c_w^2}\frac{\partial^2\Psi_w}{\partial t^2} = 0, \tag{1}$$

where ∇^2 is the Laplacian, Ψ_w is the velocity potential, and c_w is the phase speed in the fluid (seawater) medium. The equations for the compressional and shear wave in the unconsolidated sediment have been derived by Buckingham[4] by considering the stress tensor characterizing the stress relaxation arising from a microscopic, grain-to-grain sliding process in which the interaction becomes ''harder'' as the sliding progresses. For the compressional wave, the resultant equation is

$$\nabla^2\psi - \frac{1}{c_0^2}\frac{\partial^2\psi}{\partial t^2} + \frac{\lambda_h}{\rho_0 c_0^2}\frac{\partial}{\partial t}\nabla^2[h(t)\otimes\psi] + \frac{(4/3)\,\eta_h}{\rho_0 c_0^2}\frac{\partial}{\partial t}\nabla^2[h_s(t)\otimes\psi] = 0, \tag{2}$$

and for the shear wave,

$$\frac{\eta_h}{\rho_0}\nabla^2[h_s(t)\otimes\psi_s] - \frac{\partial\psi_s}{\partial t} = 0, \tag{3}$$

where ψ, ψ_s are the velocity potentials of the compressional and shear wave, respectively, c_0 is the compressional wave speed in the limit of low frequency, ρ_o is the bulk density of the sediment, and the symbol $\otimes$ denotes a temporal convolution. The coefficients λ_h and η_h are analogs of the bulk and shear viscosities, respectively, of a conventional viscous fluid. In the case of the granular sediment, these coefficients represent the effect of the slippage that occurs when grains either slide against one another (η_h) or are compressed together (λ_h). The convolution operations in Eqs. (2) and (3) allow for the fact that the stress and the strain rate associated with grain-to-grain sliding are, in general, out of phase (unlike the case of a viscous fluid, where, according to Newton's law of viscous flow for streamline motion, the stress is proportional to the strain rate). The material response functions for the compressional and shear wave, respectively, are

$$h(t) = u(t)\frac{t_0^{n-1}}{t^n}, \quad 0<n<1, \tag{4}$$

and

$$h_s(t) = u(t)\frac{t_1^{m-1}}{t^m}, \quad 0<m<1, \tag{5}$$

where the unit step function, $u(t)$, ensures that response of the medium is causal. These fractional-power functions were originally used by Nutting[11] to represent empirically the stress relaxation observed in plastic materials. Equations (4) and (5) have recently been derived by Buckingham[4] on the basis of a slip mechanism in which the grain-to-grain sliding becomes harder as the process progresses (i.e., the coefficient of the equivalent dashpot representing the grain-to-grain interaction increases with increasing time).

By Fourier transforming Eqs. (1) to (3) with respect to time, the corresponding reduced wave equations are obtained:

$$\nabla^2\Psi_w + \frac{\omega^2}{c_w^2}\Psi_w = 0, \tag{6}$$

$$\nabla^2\Psi + \frac{\omega^2}{c_0^2}\Psi + j\omega\frac{1}{\rho_0 c_0^2}\left\{\lambda_f H(j\omega) + \frac{4}{3}\eta_f H_s(j\omega)\right\}\nabla^2\Psi = 0, \tag{7}$$

and

$$\frac{\eta_f}{\rho_0}H_s(j\omega)\nabla^2\Psi_s - j\omega\Psi_s = 0, \tag{8}$$

where ω is angular frequency and the upper-case symbols, Ψ_w, Ψ, and Ψ_s, are the Fourier transforms of the corresponding lower-case velocity potentials. The Fourier-transformed material response functions are

$$H(j\omega) = \frac{\Gamma(1-n)}{(j\omega t_0)^{1-n}}, \tag{9}$$

and

$$H_s(j\omega) = \frac{\Gamma(1-m)}{(j\omega t_1)^{1-m}}. \tag{10}$$

As discussed by Buckingham,[2] when Eqs. (9) and (10) are substituted into Eqs. (7) and (8), the reduced wave equations for the sediment become

$$\nabla^2\Psi + \frac{\omega^2}{c_0^2 q^2}\Psi = 0, \tag{11}$$

and

$$\nabla^2\Psi_s + \frac{\omega^2}{c_0^2 q_s^2}\Psi_s = 0, \tag{12}$$

where

$$q = \left[1 + \frac{j\omega}{\rho_0 c_0^2}\left\{\lambda_h H(j\omega) + \frac{4}{3}\eta_h H_s(j\omega)\right\}\right]^{1/2} = \left[1 + \frac{\mu_c}{\rho_0 c_0^2}(j\omega t_0)^n + \frac{4\mu_s}{3\rho_0 c_0^2}(j\omega t_1)^m\right]^{1/2} \tag{13a}$$

and

$$q_s = \left[\frac{j\omega}{\rho_0 c_0^2}\eta_h H_s(j\omega)\right]^{1/2} = \left[\frac{\mu_s}{\rho_0 c_0^2}(j\omega t_1)\right]^{m/2}. \tag{13b}$$

In these expressions,

$$\mu_c = \lambda_h\frac{\Gamma(1-n)}{t_0} \tag{14}$$

and

$$\mu_s = \eta_h\frac{\Gamma(1-m)}{t_1}. \tag{15}$$

In effect, μ_c and μ_s are stress-relaxation rigidity moduli for the sediment. They represent the stiffness introduced by the

intergranular sliding that occurs when grains are either compressed together (μ_c) or translated relative to one another (μ_s). These two sliding processes, that is, compressional and translational, have been described in detail by Buckingham.[4]

II. BOUNDARY CONDITIONS

Across the boundary between the sediment and the overlying seawater, the normal and tangential components of stress and the normal component of particle velocity must all be continuous. Since the upper medium is a fluid, which is incapable of supporting shear, the tangential component of the stress at the boundary is zero. To derive the boundary conditions, we consider first the stress tensor for the sediment.

It is implicit in the formulation of Eqs. (2) and (3) that the elements of the stress tensor for the sediment can be expressed in the form[4]

$$\tau_{ij}=\{p-\lambda_h[h(t)\otimes \underline{v}]+\tfrac{2}{3}\,\eta_h\,\mathrm{div}[h_s(t)\otimes \underline{v}]\} - \eta_h\left[h_s(t)\otimes\left\{\frac{\partial v_i}{\partial x_j}+\frac{\partial v_j}{\partial x_i}\right\}\right], \tag{16}$$

where δ_{ij} is the Kronecker delta and p is the acoustic pressure fluctuation. This expression is the same as that for a viscous, compressible fluid,[12] except for the presence of the convolution operations involving the material response functions $h(t)$ and $h_S(t)$. Obviously, if these two material response functions were delta functions, Eq. (16) would be identical to the expression for the stress in a viscous fluid (since a function convolved with a delta function is the function itself). The normal stress and the tangential stress, as given by Eq. (16), must both be continuous across the sediment–seawater boundary.

Proceeding in standard fashion, the vector field, $\underline{v}$, is expressed from Helmholtz's theorem[13] as the sum of the gradient of a scalar (velocity) potential Ψ and the curl of a zero-divergence vector potential A as follows:

$$\underline{v}=\mathrm{grad}\,\psi+\mathrm{curl}\,\underline{A},\quad \text{where}\quad \mathrm{div}\,\underline{A}=0. \tag{17}$$

From the cylindrical symmetry of the problem, the vector potential may be expressed in cylindrical coordinates as

$$\underline{A}=-\frac{\partial \Psi_s}{\partial r}\underline{e}_\phi, \tag{18}$$

where $\underline{e}_\phi$ is the unit azimuthal vector. By combining Eqs. (16) to (18), the normal component of the stress at the boundary, in the frequency domain and in cylindrical coordinates, is found to be

$$T_{zz}|_{z=0}=-j\omega\rho_0\Psi+2\,\eta_h H_s \times\left[\frac{1}{r}\frac{\partial}{\partial r}\left(r\frac{\partial\Psi}{\partial r}\right)+\frac{1}{r}\frac{\partial^2}{\partial r\,\partial z}\left(r\frac{\partial\Psi_s}{\partial r}\right)\right] =-S\frac{\delta(r)}{2\pi r}-j\omega\rho_w\Psi_w, \tag{19}$$

where S in the first term on the far right represents the impulse of momentum applied at the surface of the sediment and the second term is the pressure in the water column immediately above the bottom. Similarly, the tangential stress at the interface is

$$T_{rz}|_{z=0}=-\eta_h H_s\frac{\partial}{\partial r}\left[2\frac{\partial\Psi}{\partial z}+2\frac{\partial^2\Psi_s}{\partial z^2}+k_s^2\Psi_s\right]=0, \tag{20}$$

where

$$k_s=\frac{\omega}{c_0 q_s} \tag{21}$$

is the complex wave number of the shear wave.

In deriving Eqs. (19) and (20), the following expressions for the Fourier-transformed radial (V_r) and normal (V_z) particle velocities in the sediment have been used:

$$V_r=\frac{\partial\Psi}{\partial r}+\frac{\partial^2\Psi_s}{\partial r\,\partial z} \tag{22}$$

and

$$V_z=\frac{\partial\Psi}{\partial z}-\frac{1}{r}\frac{\partial}{\partial r}\left(r\frac{\partial\Psi_s}{\partial r}\right). \tag{23}$$

Equations (22) and (23) are familiar forms,[14] which are derived directly from Eqs. (17) and (18). It follows from Eq. (23) that continuity of the normal component of velocity across the bottom interface requires that

$$\frac{\partial\Psi}{\partial z}-\frac{1}{r}\frac{\partial}{\partial r}\left(r\frac{\partial\Psi_s}{\partial r}\right)=\frac{\partial\Psi_w}{\partial z}\qquad \text{at } z=0. \tag{24}$$

The reduced wave equations in the preceding section, Eqs. (6), (11), and (12), are now to be solved subject to the boundary conditions expressed in Eqs. (19), (20), and (24).

III. THE CHARACTERISTIC EQUATION

When a Hankel transform of order zero is applied over horizontal range, r, to the three wave equations [Eqs. (6), (11), and (12)], each reduces to an ordinary differential equation in which the independent variable is the depth coordinate, z

$$\frac{\partial^2\Psi_{wp}}{\partial z^2}+\eta_w^2\Psi_{1p}=0, \tag{25}$$

$$\frac{\partial^2\Psi_p}{\partial z^2}+\eta^2\Psi_p=0, \tag{26}$$

and

$$\frac{\partial^2\Psi_{sp}}{\partial z^2}+\eta_s^2\Psi_{sp}=0, \tag{27}$$

where

$$\eta_w=\sqrt{k_w^2-p^2},\quad \mathrm{imag}(\eta_w)>0, \tag{28}$$

$$\eta=\sqrt{k^2-p^2},\quad \mathrm{imag}(\eta)>0, \tag{29}$$

and

$$\eta_s=\sqrt{k_s^2-p^2},\quad \mathrm{imag}(\eta_s)>0. \tag{30}$$

The wave numbers in these expressions are $k_w=\omega/c_w$, $k=k_0/q$, and $k_s=k_0/q_s$, where $k_0=\omega/c_0$, the Hankel transform variable, p, is the horizontal wave number, and the

subscript p indicates that the associated wave function is a Hankel transform. For z increasing downwards, the solutions of Eqs. (25)–(27) are

$$\Psi_{wp} = B_w \exp(-j\eta_w z), \tag{31}$$

$$\Psi_p = B \exp(j\eta z), \tag{32}$$

and

$$\Psi_{sp} = B_s \exp(j\eta_s z), \tag{33}$$

where the sign of each exponent has been chosen to ensure that the associated field goes to zero infinitely far from the interface and the three B coefficients are constants of integration which are to be determined from the boundary conditions.

When the condition in Eq. (19) on the normal stress at the boundary is Hankel transformed over range, it reduces to

$$(j\omega\rho_0 + 2\eta_h p^2 H_s)B + 2j\eta_s \eta_h p^2 H_s B_s = \frac{S}{4\pi} + j\omega\rho_w B_w, \tag{34}$$

where the expressions in Eqs. (31) to (33) have been substituted for the various field terms. Similarly, on Hankel transforming the condition on the tangential stress in Eq. (20), the result

$$2j\eta B - 2\eta_s^2 B_s + k_s^2 B_s = 0 \tag{35}$$

is obtained. In fact, to derive this expression a Hankel transform of first order was applied to Eq. (20), since the first-order transform of the derivative of a function is equivalent to the zero-order transform of the function itself. Finally, the third of the boundary conditions, on the normal component of velocity in Eq. (24), yields, after a zero-order Hankel transform,

$$j\eta B + p^2 B_s = -j\eta_w B_w. \tag{36}$$

Equations (34)–(36) are a set of simultaneous equations that may be solved for the coefficients B, B_w, and B_s. The results are as follows:

$$B = \frac{S}{4\pi}\frac{(2\eta_s^2 - k_s^2)}{D}, \tag{37}$$

$$B_s = \frac{S}{4\pi}\frac{2j\eta}{D}, \tag{38}$$

and

$$B_w = -\frac{S}{4\pi}\frac{\eta}{\eta_w D}[2\eta_s^2 - k_s^2 + 2p^2]. \tag{39}$$

The term D appearing in the denominator of each of these expressions is

$$D = \left(j\omega\rho_0 + 2\eta_h p^2 H_s + j\omega\rho_w \frac{\eta}{\eta_w}\right)(2\eta_s^2 - k_s^2) - 4\eta\eta_s\eta_h p^2 H_s + 2j\omega\rho_w p^2 \frac{\eta}{\eta_w}. \tag{40}$$

Thus, D is a function of p, the integration variable of the inverse Hankel transform that must be applied to Eqs. (31)–(33) in order to obtain the frequency-domain velocity potential in the water column and the compressional and shear fields in the sediment. A zero of D corresponds to a pole in the complex p-plane and one of these poles represents an interface wave propagating along the water–sediment boundary. Notice that D does not depend on the bulk material response function, H.

To investigate the pole representing the interface wave, it is necessary to find the corresponding (complex) root of D, that is, to solve the characteristic equation

$$D = 0. \tag{41}$$

It is convenient to make the substitution

$$u^2 = -\frac{j\omega\rho_0}{\eta_h H_s} = \frac{\omega^2\rho_0 t_0}{\eta_h \Gamma(1-m)(j\omega t_1)^m}, \tag{42}$$

in which case the characteristic equation can be expressed as

$$(2p^2 - u^2)(k_s^2 - 2p^2) + \frac{j\omega\rho_w\sqrt{k^2 - p^2}}{\eta_h H_s \sqrt{k_w^2 - p^2}} k_s^2 - 4p^2\sqrt{k^2 - p^2}\sqrt{k_s^2 - p^2} = 0, \tag{43}$$

where b is the density ratio

$$b = \frac{\rho_w}{\rho_0} < 1. \tag{44}$$

Equation (43) may be further simplified by letting

$$x = \frac{k^2}{k_s^2}, \tag{45a}$$

$$y = \frac{u^2}{k_s^2} = 1, \tag{45b}$$

and

$$w = \frac{k_w^2}{k_s^2}, \tag{45c}$$

to obtain

$$4\sqrt{1-xs}\sqrt{1-s} - (s-2)(sy-2) - bs^2 y\sqrt{\frac{1-xs}{1-ws}} = 0, \tag{46}$$

which, since y is identically equal to unity, is equivalent to

$$4\sqrt{1-xs}\sqrt{1-s} - (s-2)^2 - bs^2\sqrt{\frac{1-xs}{1-ws}} = 0. \tag{47}$$

The variable s, as defined in Eq. (45a), is a measure of the (complex) interface wave speed relative to the (complex) shear wave speed in the sediment. Before solving for s, it is worth commenting that the characteristic equation in Eq. (47) is identical in form to that for an elastic solid overlain by a fluid.[15] In other words, the characteristic equation for the pseudo-Scholte wave in Eq. (47) is exactly the same as the corresponding equation for a true Scholte wave,[16] even though the underlying physical mechanisms giving rise to the two types of interface wave are completely different. Notice that for the special case when $b = 0$, representing the situation where the fluid medium is a vacuum, Eq. (47) re-

duces identically to the characteristic equation for a Rayleigh wave.

IV. COMPLEX-ROOT FINDING

In the absence of attenuation, all the parameters in Eq. (47) are real, a real solution for s exists which is positive and less than unity and which may be found using an iterative Newton–Raphson procedure. This real root yields the phase speed of the interface wave relative to the shear-wave speed. When attenuation in the sediment is present, however, the required root becomes complex, in which case the Newton–Raphson algorithm cannot be applied directly, indicating that some alternative method must be employed.

Rather than turn to a complex-root-finding algorithm, an approximate approach is introduced here, which is based on the observation that, for unconsolidated marine sediments, the imaginary parts of all the complex variables in Eq. (47) are very much smaller than the corresponding real parts. Indicating the real and imaginary parts by single and double primes, respectively, we have

$$s = s' + js'', \quad s'' \ll s', \tag{48a}$$

$$x = x' + jx'', \quad x'' \ll x', \tag{48b}$$

and

$$w = w' + jw'', \quad w'' \ll w'. \tag{48c}$$

Similarly, the characteristic equation may be written as

$$D = D' + jD'' = 0, \tag{49}$$

which is satisfied only if the real (D') and imaginary (D'') parts are individually equal to zero.

When the expressions in Eqs. (48) are substituted into Eq. (47), we find that D' and D'' are, to first order in the small imaginary terms, as follows:

$$D' = 4\sqrt{1-x's'}\sqrt{1-s'} - (s'-2)^2 - bs'^2\sqrt{\frac{1-x's'}{1-w's'}} = 0 \tag{50a}$$

and

$$D'' = -As'' - B = 0, \tag{50b}$$

where

$$A = 2x'\frac{\sqrt{1-s'}}{\sqrt{1-x's'}} + 2\frac{\sqrt{1-x's'}}{\sqrt{1-s'}} + 2(s'-2)^2 + 2bs'\sqrt{\frac{1-x's'}{1-w's'}} - \frac{bs'^2x'}{2\sqrt{1-w's'}\sqrt{1-x's'}} + \frac{bs'^2w'\sqrt{1-x's'}}{2(1-w's')^{3/2}} \tag{50c}$$

and

$$B = 2x''s'\frac{\sqrt{1-s'}}{\sqrt{1-x's'}} - \frac{bs'^3x''}{2\sqrt{1-w's'}\sqrt{1-x's'}} + \frac{bs'^3w''\sqrt{1-x's'}}{2(1-w's')^{3/2}}. \tag{50d}$$

Obviously, from Eq. (50b) the solution for the imaginary part of s is

$$s'' = -\frac{B}{A}. \tag{51}$$

Equation (50a) is simply the characteristic equation that holds in the absence of attenuation. It may be solved numerically for the real root, s', which lies between zero and unity, using a standard, iterative Newton–Raphson procedure. Once s' has been determined in this way, the imaginary part of s may be evaluated from Eq. (51), since all the terms in A and B are then known. Thus, Eqs. (50a) and (51) provide a means of solving for s' and s'', from which the interface wave speed and attenuation may be determined.

V. INTERFACE WAVE SPEED AND ATTENUATION

From Eq. (45a), the (complex) wave number of the interface wave is

$$p = \frac{k_s}{\sqrt{s}} = \frac{\omega}{c_o q_s \sqrt{s}}, \tag{52}$$

where q_s is given by Eq. (13b). Now, p can be expressed in the form

$$p = \frac{\omega}{c_i}(1 - j\beta_i), \tag{53}$$

where c_i and β_i are, respectively, the phase speed and the loss tangent of the interface wave. On comparing Eqs. (52) and (53), it follows that

$$\frac{1}{c_i} = \frac{1}{c_o}\mathrm{Re}\left[\frac{1}{q_s\sqrt{s}}\right] = \mathrm{Re}\sqrt{\frac{\rho_o}{\mu_s s(j\omega t_1)^m}} \tag{54}$$

and

$$\beta_i = -\frac{c_i}{c_o}\mathrm{Im}\left[\frac{1}{q_s\sqrt{s}}\right] = -c_i\,\mathrm{Im}\left[\frac{\rho_o}{\mu_s s(j\omega t_1)^m}\right]^{1/2}. \tag{55}$$

As $m \ll 1$ and $s'' \ll s'$, Eq. (54) may be approximated as follows:

$$c_i \approx \sqrt{\frac{\mu_s}{\rho_o}s'} \approx c_s\sqrt{s'}, \tag{56}$$

where c_s is the speed of the shear wave in the granular medium

$$\frac{1}{c_s} = \frac{1}{c_0}\mathrm{Re}\left[\frac{1}{q_s}\right] \approx \sqrt{\frac{\rho_o}{\mu_s}}. \tag{57}$$

Similarly, the loss tangent in Eq. (55) approximates to

$$\beta_i \approx \frac{s''}{2s'} + \frac{m\pi}{4}, \tag{58}$$

and obviously the attenuation coefficient, α_i, of the interface wave can be calculated from Eqs. (57) and (58), since

$$\alpha_i = \frac{|\omega|\beta_i}{c_i}. \tag{59}$$

VI. GRAIN-SIZE DEPENDENCIES

It is evident from Eqs. (56)–(59) that the wave properties of the interface wave depend on μ_c and μ_s, both of which vary with the grain size. The functional forms of these grain-size dependencies have been developed by Buckingham[1,2] on the basis of the Hertz theory of elastic spheres pressed together in contact.[17] The properties of the interface wave also depend on c_0, the wave speed in the sediment in the limit of low frequency, and on the sediment density ρ_0. Both c_0 and ρ_0 are functions of the porosity, N, which itself depends on the grain size, as discussed by Buckingham on the basis of a random-packing model of rough spheres in contact. Since these grain-size dependencies have been established in the cited papers, they are not redeveloped here, instead, the results are simply stated.

The stress-relaxation rigidity moduli increase with grain size, as given by the following fractional-power relationships

$$\mu_c = \mu_0 \left(\frac{u_g}{u_0} \right)^{1/3} \tag{60}$$

and

$$\mu_s = \mu_1 \left(\frac{u_g}{u_0} \right)^{2/3}, \tag{61}$$

where $\mu_0 = 2 \times 10^9$ Pa, $\mu_1 = 5.1 \times 10^7$ Pa, $u_0 = 1000\,\mu$m, and u_g is the mean grain diameter in micrometers. For coarse sand, with a grain diameter $u_g \approx 700\,\mu$m, and for all finer marine sediments, $\mu_c \gg \mu_s$. As an example, a medium sand with $u_g \approx 400\,\mu$m shows $\mu_c \approx 1.5 \times 10^9$ Pa and $\mu_s \approx 2.8 \times 10^7$ Pa, a difference of almost two orders of magnitude.

The porosity of the sediment, as given by the random-packing model of rough, spherical particles in contact is

$$N = 1 - P \left\{ \frac{u_g + 2\Delta}{u_g + 4\Delta} \right\}^3, \tag{62}$$

where $P = 0.63$ is the packing factor of a random arrangement of smooth spheres,[18] and Δ is the rms roughness of the grains, as measured about the mean surface of a particle. A value of $\Delta = 3\,\mu$m, independent of grain size, provides a reasonable description of surficial, unimodal, sandy sediments.

The density, ρ_0, and bulk modulus, κ_0, of the sediment are given by the following weighted means:

$$\rho_0 = N\rho_w + (1-N)\rho_g \tag{63}$$

and

$$\frac{1}{\kappa_0} = N \frac{1}{\kappa_w} + (1-N) \frac{1}{\kappa_g}, \tag{64}$$

where the densities and bulk moduli of the constitutive mineral grains and seawater are: $\rho_g = 2700\,\text{kg/m}^3$, $\kappa_g = 1.47 \times 10^{10}$ Pa, $\rho_w = 1024\,\text{kg/m}^3$, and $\kappa_w = 2.25 \times 10^9$ Pa. The sound speed in the absence of intergranular stress relaxation is therefore

$$c_0 = \sqrt{\frac{\kappa_0}{\rho_0}} = \sqrt{\frac{\kappa_w \kappa_g}{[N\rho_w + (1-N)\rho_g][N\kappa_g + (1-N)\kappa_w]}}, \tag{65}$$

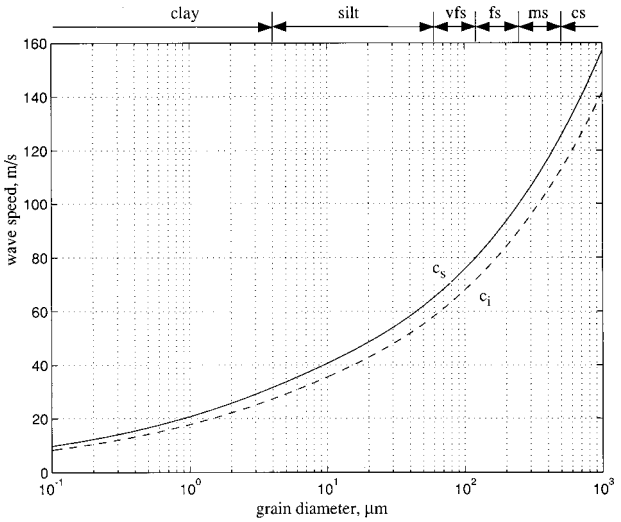

FIG. 2. Wave speeds as a function of grain size. The symbols at the top of the graph denote very fine sand (vfs), fine sand (fs), medium sand (ms), and coarse sand (cs).

which is just Wood's equation[19] for the sound speed in a two-phase medium. In effect, c_0 is the sound speed in the sediment that would be observed if the medium were a suspension, with no interaction between the grains.

Based on Eqs. (56) and (57), in conjunction with the expressions given above, the grain-size dependencies of c_i and c_s are shown in Fig. 2, and the ratio of c_i to c_s as a function of the grain diameter is plotted in Fig. 3. It is evident from Fig. 3 that the ratio c_i/c_s depends only weakly on grain size, increasing by about 5%, from 85% to 90%, over the three decades of grain diameter between 1 and 1000 micrometers.

From the attenuation of shear waves in medium sand (with grain diameters between 350 and 380 μm), as measured under laboratory conditions by Brunson and Johnson[7] and Brunson,[8] Buckingham[2] has estimated that $m \approx 0.05$.

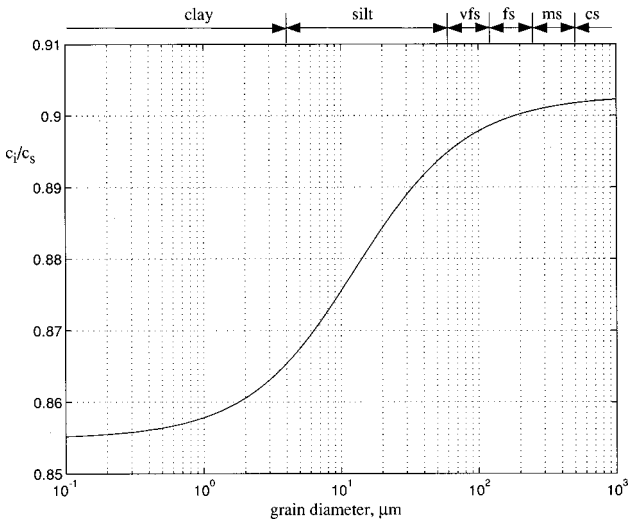

FIG. 3. Interface wave speed relative to shear wave speed as a function of grain size. The variation in the curve arises entirely from the density ratio, b, between the water column and the sediment, which varies with grain size. The key to the symbols at the top of the graph is given in the legend to Fig. 2.

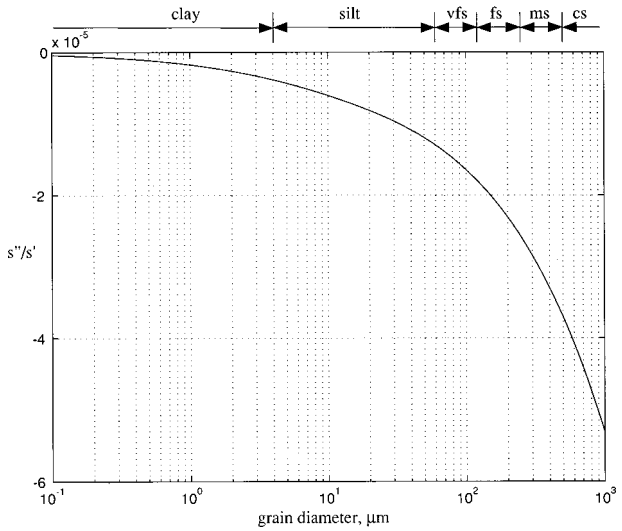

FIG. 4. Ratio of the imaginary to real part of s as a function of grain size. The key to the symbols at the top of the graph is given in the legend to Fig. 2.

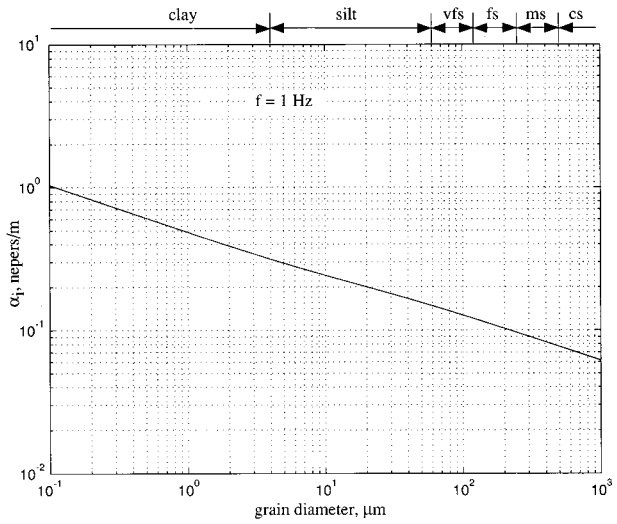

FIG. 5. Attenuation coefficient, α_i, as a function of grain size. The key to the symbols at the top of the graph is given in the legend to Fig. 2.

With this value for the shear material response index m, it turns out, as shown in Fig. 4, that the ratio $s''/2s'$ is negligible compared with the last term in Eq. (57); that is,

$$\beta_i \approx \frac{m\pi}{4}. \tag{66}$$

Evidently, to this degree of approximation, the loss tangent of the interface wave is equal to the loss tangent of the shear wave.[2] Both loss tangents scale with m, the material response index for shear, but are essentially independent of the remaining sediment parameters (e.g., the grain size, density, and porosity). With $m=0.05$, the value of the loss tangent for the pseudo-Scholte wave from Eq. (66) is $\beta_i \approx 0.04$. Incidentally, the value of the material response index for compressional waves is $n \approx 0.05$, as estimated by Buckingham[1] from comparison with attenuation data for unconsolidated marine sediments reported by Hamilton.[5] It would seem from these estimates that, tentatively, we have $m \approx n$.

The attenuation coefficient, α_i, of the interface wave may now be computed directly from Eq. (59). Since β_i and c_i are independent of frequency, at least to the level of approximation in Eqs. (56) and (66), the attenuation coefficient of the interface wave is directly proportional to frequency. This is the same type of frequency dependence exhibited by the attenuation coefficient of the compressional wave and the shear wave. Note that α_i depends on the grain size primarily through the phase speed c_i, which is a function of the stress-relaxation modulus μ_s, as given in Eq. (61).

Figure 5 shows the attenuation coefficient, α_i, as a function of grain size for a frequency of 1 Hz, computed using the expressions in Eqs. (56), (57), (59), and (66). The material response index has been taken as $m=0.05$, since this value is consistent with measurements of the shear attenuation in sands,[1,2] as discussed above. Note that the attenuation of the pseudo-Scholte wave in Fig. 5 is highest in the fine-grained materials and decays monotonically with increasing grain size, a dependence that arises almost entirely from the increase of phase speed, c_i, with grain size. This increase in phase speed, c_i, and the reduction in attenuation, α_i, with increasing grain size are indicative of the higher stiffness exhibited by the coarser-grained materials.

VII. COMPARISON WITH INTERFACE-WAVE ATTENUATION DATA

A number of experiments on the interface wave propagating along the seawater–sediment boundary have been reported in the literature.[20–34] In many of these experiments, the frequency of the interface wave was well below 10 Hz, implying that the evanescent tail of the wave penetrated several tens of meters into the sediment, where the strong shear-speed gradient introduced significant dispersion. The presence of this type of dispersion makes it difficult to compare these measurements of wave speed and attenuation with the predictions of the theory [Eqs. (56) and (59)], since the latter apply to the case of a homogeneous, isotropic sediment in which the compressional speed and shear speed show no dispersion associated with wave speed profiles.

Two groups of investigators,[20,29] however, have reported observations of the phase speed and attenuation of interface waves with a frequency of 20 Hz or greater, where the effects of profile-related dispersion are rather less pronounced (see Fig. 4 in Ref. 29). Both groups used a line of seismometers on a sandy seabed to detect the signals generated by an explosive or vibrating source placed close to the end of the line. Propagation ranges were of the order of several meters. Table I lists some of the details of these experiments, including the frequency of the interface wave, the observed wave speed, and the measured attenuation coefficient, which has been converted to the equivalent loss tangent. Notice that the three measured loss tangents all agree, within the limits of experimental error, with the theoretical value, $\beta_i \approx 0.04$, derived above for the pseudo-Scholte wave.

In similar experiments conducted by Hamilton *et al.*,[23] broadband sources (electrical detonators) were used to generate interface waves in various types of marine sediment. No attenuation data for the interface waves were reported

TABLE I. Measured phase speed and attenuation of the interface wave in sandy sediments.

Investigators	Sediment type	Frequency (Hz)	Phase speed (m/s)	Attenuation (dB/m)	Loss tangent (β)
Bucker *et al.* (Ref. 20)	sand	20	90	0.33 ± 0.16	0.027 ± 0.013
Bucker *et al.* (Ref. 20)	sand	25	172	0.2 ± 0.13	0.025 ± 0.017
Holt *et al.* (Ref. 29)	sand	35	120	0.6 ± 0.2	0.038 ± 0.012

directly, but it was observed by these authors that ''Most of the spectral energy of the Stoneley waves was at frequencies less than 100 Hz...'' over propagation path lengths of the order of several meters. This limited bandwidth may be interpreted in terms of the expression for the attenuation of the pseudo-Scholte wave in Eq. (59), as discussed below.

Defining the cutoff in the detected signal by the *e*-folding frequency, f_e, at which the product of the attenuation coefficient, α_i, and the range, r, is equal to unity, it follows from Eq. (59) that

$$f_c=\frac{c_i}{2\pi r\beta_i}. \tag{67}$$

At the Tower site used by Hamilton *et al.*,[23] the range between the source and the farthest receiver was $r=14.3$ m, and the sediment was medium sand with a measured interface wave speed of $c_i=170$ m/s. Thus, with $\beta_i\approx0.04$, the *e*-folding frequency from Eq. (67) is $f_e\approx47.3$ Hz, which is consistent with the restricted bandwidths observed in the experiment. Similarly, for the other five sites investigated by Hamilton *et al.*,[23] where the maximum source–receiver range was 6.3 m, the *e*-folding frequencies are $f_e=56.2(89)$, 59.4(94), 48(76), 84(133), and 77.7(123) Hz. The numbers in parentheses are the reported interface wave speeds in m/s. Again, these *e*-folding frequencies are all less than 100 Hz, suggesting that attenuation in the sediment was largely responsible for the restricted bandwidths observed in these experiments.

VIII. CONCLUDING REMARKS

The characteristic equation for the interface (pseudo-Scholte) wave at the seawater–sediment boundary has been derived on the assumption that stress relaxation in the sediment arises at grain boundary contacts. The particular type of stress relaxation considered is characterized by material response functions of the form $h(t)\propto t^{-n}$, where n is positive but small compared with unity. Since the sediment is a dissipative medium, the required root of the characteristic equation is complex, and this root yields the phase speed and the attenuation of the interface wave. To solve for this complex root, an approximate technique is introduced in which the characteristic equation is split into two separate equations, one of which can be solved numerically for the real part of the root. Once the real part has been obtained, it may be substituted into the second equation, which then yields the imaginary part directly. An essential requirement of this technique is that the imaginary parts of all the complex variables in the characteristic equation must be very much smaller than the corresponding real parts, a condition that is easily satisfied by unconsolidated marine sediments.

The phase speed of the interface wave turns out to be weakly dependent on grain size, taking a value between 85% and 90% of the shear wave speed. In fact, the interface wave speed relative to the shear wave speed is the same as if the sediment were an elastic solid of the same density. In other words, Eq. (56) is identical to the relationship between the shear wave speed and the interface wave speed in an elastic medium. This is an important observation, because a number of authors, including Hamilton *et al.*,[23] have performed measurements of the interface wave speed from which they computed the shear wave speed on the assumption that the seabed was an elastic solid. Their results would have remained unchanged if they had used the expression in Eq. (56), derived from the stress-relaxation theory, to compute the shear wave speed. This is not to say that a marine sediment actually acts as an elastic solid. The elastic description fails on a number of counts, including the fact that it does not yield the grain-size dependencies exhibited by the compressional and shear wave speeds.[4]

The attenuation coefficient of the pseudo-Scholte wave that emerges from the stress-relaxation analysis is proportional to the first power of frequency. The corresponding loss tangent is thus independent of frequency, and its value turns out to be essentially the same as that predicted for the shear wave in the sediment. Little information on the attenuation of interface waves in marine sediments is available in the literature, at least for frequencies where dispersion due to a shear speed profile is negligible, but, within the limits of experimental error, the data that have been reported are in agreement with the theoretically derived attenuation coefficient. Moreover, the spectral content of interface wave arrivals on the seabed, as observed by Hamilton *et al.*,[23] is consistent with the predictions of the stress-relaxation theory.

[1] M. J. Buckingham, ''Theory of acoustic attenuation, dispersion, and pulse propagation in unconsolidated granular materials including marine sediments,'' J. Acoust. Soc. Am. **102**, 2579–2596 (1997).
[2] M. J. Buckingham, ''Theory of compressional and shear waves in fluid-like marine sediments,'' J. Acoust. Soc. Am. **103**, 288–299 (1998).
[3] M. J. Buckingham, ''Theory of compressional and transverse wave propagation in consolidated porous media,'' J. Acoust. Soc. Am. **106**, 575–581 (1999).
[4] M. J. Buckingham, ''Wave propagation, stress relaxation, and grain-boundary interactions in saturated, unconsolidated marine sediments,'' J. Acoust. Soc. Am. (submitted).
[5] E. L. Hamilton, ''Compressional-wave attenuation in marine sediments,'' Geophysics **37**, 620–646 (1972).
[6] E. L. Hamilton, ''Acoustic properties of sediments,'' in *Acoustics and the Ocean Bottom* (Consejo Superior de Investigacions Cientificas, Madrid, (1987), pp. 3–58.
[7] B. A. Brunson and R. K. Johnson, ''Laboratory measurements of shear wave attenuation in saturated sand,'' J. Acoust. Soc. Am. **68**, 1371–1375 (1980).
[8] B. A. Brunson, ''Shear wave attenuation in unconsolidated laboratory

sediments,'' in *Shear Waves in Marine Sediments* (Kluwer, Dordrecht, 1991), pp. 141–147.
[9] M. N. Toksöz and D. H. Johnston, *Seismic Wave Attenuation* (Society of Exploration Geophysicists, Tulsa, OK, 1981), p. 459.
[10] W. L. Roever, T. F. Vining, and E. Strick, ''Propagation of elastic wave motion from an impulsive source along a fluid/solid interface. I. Experimental pressure response. II. Theoretical pressure response. III. The pseudo-Rayleigh wave,'' Philos. Trans. R. Soc. London, Ser. A **251**, 455–523 (1959).
[11] P. Nutting, ''A study of elastic viscous deformation,'' Proceedings of the American Society for Testing Materials XXI (1921), pp. 1162–1171.
[12] P. M. Morse and K. U. Ingard, *Theoretical Acoustics* (McGraw-Hill, New York, 1968), p. 927.
[13] P. M. Morse and H. Feshbach, *Methods of Theoretical Physics: Part 1* (McGraw-Hill, New York, 1953), p. 997.
[14] K. F. Graff, *Wave Motion in Elastic Solids* (Dover, New York, 1975), p. 649.
[15] L. M. Brekhovskikh, *Waves in Layered Media* (Academic, San Diego, 1980), p. 503.
[16] J. G. Scholte, ''Over het verband tussen zeegolven en microseismen, I and II,'' Verslag. Ned. Akad. Wet. **52**, 669–683 (1943).
[17] S. P. Timoshenko and J. N. Goodier, *Theory of Elasticity* (McGraw-Hill, New York, 1970), p. 567.
[18] O. K. Rice, ''On the statistical mechanics of liquids, and the gas of hard elastic spheres,'' J. Chem. Phys. **12**, 1–18 (1944).
[19] A. B. Wood, *A Textbook of Sound* (G. Bell and Sons Ltd., London, 1964), p. 610.
[20] H. P. Bucker, J. A. Whitney, and D. L. Keir, ''Use of Stoneley waves to determine the shear velocity in ocean sediments,'' J. Acoust. Soc. Am. **36**, 1595–1596 (1964).
[21] D. Davies, ''Dispersed Stoneley waves on the ocean bottom,'' Bull. Seismol. Soc. Am. **55**, 903–918 (1965).
[22] E. M. Herron, J. Dorman, and C. L. Drake, ''Seismic study of the sediments in the Hudson River,'' J. Geophys. Res. **73**, 4701–4709 (1968).
[23] E. L. Hamilton, H. P. Bucker, D. L. Keir, and J. A. Whitney, ''Velocities of compressional and shear waves in marine sediments determined in situ from a research submersible,'' J. Geophys. Res. **75**, 4039–4049 (1970).
[24] D. Rauch, ''Experimental and theoretical studies of seismic interface waves in coastal waters,'' in *Bottom-Interacting Ocean Acoustics* (Plenum, New York, 1980), pp. 307–327.
[25] F. Schirmer, ''Experimental determination of properties of the Scholte wave in the bottom of the North Sea,'' in *Bottom-Interacting Ocean Acoustics* (Plenum, New York, 1980), pp. 285–298.
[26] H. H. Essen, H. Janle, F. Schirmer, and J. Siebert, ''Propagation of surface waves in marine sediments,'' J. Geophys. **49**, 115–122 (1981).
[27] J. D. Tuthill, B. R. Lewis, and J. D. Garmany, ''Stoneley waves, Lopez Island noise, and deep sea noise from 1 to 5 Hz,'' Mar. Geophys. Res. **5**, 95–108 (1981).
[28] T. M. Brocher, B. T. Iwatake, and D. A. Lindwall, ''Experimental studies of low-frequency waterborne and sediment-borne acoustic wave propagation on a continental shelf,'' J. Acoust. Soc. Am. **74**, 960–972 (1983).
[29] R. M. Holt, J. M. Hovem, and J. Syrstad, ''Shear modulus profiling of near bottom sediments using boundary waves,'' in *Acoustics and the Sea-Bed* (Bath University Press, Bath, 1983), pp. 317–325.
[30] D. Rauch and B. Schmalfeldt, ''Ocean-bottom interface waves of the Stoneley/Scholte type: properties, observations and possible use,'' in *Acoustics and the Sea-Bed* (Bath University Press, Bath, 1983), pp. 307–316.
[31] B. Schmalfeldt and D. Rauch, *Explosion-Generated Seismic Interface Waves in Shallow Water: Experimental Results*, SACLANT ASW Research Centre, La Spezia, Report SR-71 (1983).
[32] D. Rauch, ''On the role of bottom interface waves in ocean seismo-acoustics: a review,'' in *Ocean Seismo-Acoustics* (Plenum, New York, 1986), pp. 623–641.
[33] D. M. F. Chapman and P. R. Staal, ''A summary of DREA observations of interface waves at the seabed,'' in *Shear Waves in Marine Sediments* (Kluwer, Dordrecht, 1991), pp. 177–184.
[34] G. Nolet and L. M. Dorman, ''Waveform analysis of Scholte modes in ocean sediment layers,'' Geophys. J. Int. **125**, 385–396 (1996).